

# The effects of drift and winds on the propagation of Galactic cosmic rays

A. AL-Zetoun<sup>1\*</sup> & A. Achterberg<sup>1</sup>

<sup>1</sup>*Department of Astrophysics, IMAPP, Radboud University, Nijmegen, P.O. Box 9010, 6500 GL Nijmegen, The Netherlands*

Accepted..., Received...; in original form ...

## ABSTRACT

We study the effects of drift motions and the advection by a Galactic wind on the propagation of cosmic rays in the Galaxy. We employ a simplified magnetic field model, based on (and similar to) the Jansson-Farrar model for the Galactic magnetic field. Diffusion is allowed to be anisotropic. The relevant equations are solved numerically, using a set of stochastic differential equations. Inclusion of drift and a Galactic wind significantly shortens the residence time of cosmic rays, even for moderate wind speeds.

**Key words:** Methods: numerical – diffusion – magnetic fields – cosmic rays – supernova remnants

## 1 INTRODUCTION

Cosmic rays (CRs) propagate in the Galaxy and through the surrounding halo around the Galactic disk by a combination of diffusion, drift through the ambient magnetic field and advection by a large-scale wind e.g. [Strong et al. \(2007\)](#). These processes are usually studied using by solving a diffusion-advection equation. In addition CRs can gain (through re-acceleration) or lose (through expansion losses in a wind) energy during propagation. During propagation CR composition is changed due to spallation on ISM nuclei or by radioactive decay of unstable nuclei.

The charged CR nuclei (and CR electrons and positrons) are collisionally coupled to a possible Galactic wind, causing them to be advected by the bulk flow, see for instance [Skilling \(1975\)](#). This coupling is due to frequent scattering of the CRs as a result of wave-particle interactions with low-frequency MHD waves. The intensity of these waves is determined by the CR density gradient, which causes the excitation of Alfvén waves, see [Wentzel \(1974\)](#) or [Skilling \(1975\)](#).

The mechanisms driving a Galactic winds include the deposition of mechanical energy into the ISM by core collapse supernovae, see for instance [Martin \(1999\)](#), and the effects of radiation- or CR pressure e.g. [Hopkins et al. \(2012\)](#). The effect of such a large-scale wind is now routinely included in numerical simulations of CR propagation.

In the diffuse Galactic disk there is a rough equipartition of the CR energy density and the energy density of the Galactic magnetic field, see for example [Beck & Krause \(2005\)](#). This implies that CRs can play a significant role in the dynamics of the ISM. That last point will not be addressed in this paper.

CR drift motions with respect of the large-scale magnetic field are usually a combination of gradient and curvature drifts. These are indispensable ingredients in the study the CR propagation in the Galaxy and (on a much smaller scale) in the Solar Wind. For example: [Jokipii et al. \(1977\)](#) has presented a model of CR propagation in the solar wind that includes drift. Those authors studied the effects of gradient drifts on CR transport, with the magnetic field taken to be an Archimedean spiral.

In this paper we take into account the effects of cross-field drift in the curved magnetic field, and the effects of CR advection away from the disk by the Galactic winds on the propagation of CRs in the Galaxy.

A number of analytical models for the Galactic magnetic field have been published in recent years, see for instance: [Sun et al. \(2008\)](#), [Jaffe et al. \(2010\)](#), and [\(Jansson & Farrar 2012a,b\)](#).

\* E-mail: a.al-zetoun@astro.ru.nl

The (Jansson & Farrar 2012a,b) model, hereafter JF12, *does* include a detailed model for the vertical field. In this paper we use a simplified GMF model (see below), based on JF12 model. This model preserves most of the features of the JF12 model: the field in the plane of the disk (horizontal field) is essentially unchanged, but, close to the disk mid-plane, the vertical field is taken to be perpendicular to the Galactic disk. The reason for this approach is mainly that the simplified model, unlike the original JF12 model, allows a (relatively) simple analytical calculation of CR drifts, which can then be used to check the numerical results.

The reason for this approach is mainly that the simplified model, unlike the original JF12 model, allows a (relatively) simple analytical calculation of CR drifts. These analytical results, summarized in the Appendix, are used to calculate the drift speed in the advective step. Other than the inclusion of CR drift and advection by a Galactic wind, the numerical methods used in this Paper are identical to those used in the two previous papers (AL-Zetoun & Achterberg (2018), and AL-Zetoun & Achterberg (2020)). As a result, the performance and efficiency of the code is comparable to what was found before.

The rest of the paper is organized as follows: In Section 2.1, we describe the large scale Galactic magnetic field model. We discuss our propagation model using relevant input, like the diffusion tensor, the path length and the grammage distribution, advection by Galactic wind, and drift velocity in Section 2.2, 2.3, and 2.4, respectively. In Section 3 we discuss the spatial distribution of CRs in the Galaxy when we include the drift motion and the advection by Galactic wind. Finally, Section 4 contains the conclusions. In the Appendix we give the details of the CR drift in the modified Jansson-Farrar field.

## 2 SIMULATION ASSUMPTIONS AND PARAMETERS

### 2.1 the Galactic magnetic field model

We briefly discuss our modification of the GMF model of Jansson & Farrar (2012a) and Jansson & Farrar (2012b). The JF12 model has three distinct components: spiral disk field, a poloidal X-shaped field, and a toroidal halo field. Our simplifications involve the disk component as well as the *X-field* component, as explained immediately below.

- (i) For a distance  $|z| \leq h = 0.4$  kpc from the disk mid-plane we take the field to be

$$\mathbf{B}(r) = B_0^D \left( \frac{r_0}{r} \right) (\sin p \hat{\mathbf{r}} + \cos p \hat{\boldsymbol{\phi}}) + B_0^X \exp(-r_p/H_X) \sin i(r_p) \hat{\mathbf{z}}. \quad (1)$$

Here the first term is the spiral field in the disk plane, while the second term is the vertical X-field. The spiral pitch angle  $p = 11.5$  degrees and the value of  $B_0^D$  is different in the 8 spiral sections of the field. The disk field scales with Galacto-centric radius  $r$  as:  $\mathbf{B}^D \propto r^{-1}$ , the radius  $r_0$  can be chosen arbitrarily, in our simulations we use the value of  $r_0 = 5$  kpc, see Jansson & Farrar (2012a) and AL-Zetoun & Achterberg (2018) for details. We take the *X-field* to be purely vertical with the same properties as the vertical component of the JF12 field:  $B_0^X = 4.6 \mu\text{G}$ ,  $H_X = 2.9$  kpc, and  $\tan i(r_p) = (r_X/r_p) \tan i_0$  for  $r_p < r_X = 4.8$  kpc and  $\tan i(r_p) = \tan i_0$  for  $r_p \geq r_X$ . Here  $r_p = r/(1 + h/r_X \tan i_0)$  for  $r_p < r_X$  and  $r_p = r - h/\tan i_0$  for  $r_p \geq r_X$  and  $\tan i_0 = 1.15$  ( $i_0 = 49$  degrees).

- (ii) For  $|z| > h$  we assume that the disk field vanishes abruptly. In the JF12 model this transition is more gradual. The X-field remains in the form given in Jansson & Farrar (2012a):

$$\mathbf{B}(r) = B^X(r_p) \cos(i) \hat{\mathbf{r}} + B^X(r_p) \sin(i) \hat{\mathbf{z}}. \quad (2)$$

We neglect the relatively weak halo field.

### 2.2 The equations for CR propagation

Recently, AL-Zetoun & Achterberg (2018) presented the results from a fully three-dimensional simulation of CR propagation, based on the Itô formulation of the Fokker Planck in terms of a set of stochastic differential equations. The results allowed for anisotropic diffusion but neglected the effects of CR drift and the Galactic wind. In this paper we include these effects.

In finite-difference form the Itô formulation advances the position  $\mathbf{x}$  of a simulated CR as the sum of a regular advective step and a diffusive stochastic (random) step. In a time span  $\Delta t$  one has

$$\Delta \mathbf{x} = (\mathbf{V}_w(\mathbf{x}) + \mathbf{V}_{\text{dr}}(\mathbf{x})) \Delta t + \Delta \mathbf{x}_{\text{diff}}. \quad (3)$$

The proper definitions of the wind speed  $\mathbf{V}_w$  and the drift speed  $\mathbf{V}_{dr}$  are given directly below. The diffusive step  $\Delta \mathbf{x}_{diff}$  has the form:

$$\Delta \mathbf{x}_{diff} = \sqrt{2D_{\perp} \Delta t} \xi_1 \hat{e}_1 + \sqrt{2D_{\perp} \Delta t} \xi_2 \hat{e}_2 + \sqrt{2D_{\parallel} \Delta t} \xi_3 \hat{e}_3, \quad (4)$$

It involves Gaussian random steps with rms size  $\sqrt{2D_{\parallel} \Delta t}$  in the direction along the magnetic field, and random steps with rms size  $\sqrt{2D_{\perp} \Delta t}$  in the two directions in the plane perpendicular to the magnetic field. For more details about these aspects of the model, see [AL-Zetoun & Achterberg \(2018\)](#). To achieve this, the random variables  $\xi_1$ ,  $\xi_2$  and  $\xi_3$  are independently drawn from a Gaussian distribution with zero mean and unit dispersion. In our simulations we use a constant value for the ratio  $D_{\perp}/D_{\parallel} \equiv \epsilon$ . The scaling with CR rigidity  $\mathcal{R} = pc/qB$  is  $D_{\parallel} \propto \mathcal{R}^{\delta}$ . Values quoted for  $D_{\parallel}$  are for protons with an energy of 1 GeV.

### 2.3 Path length and the grammage distribution

The path length distribution (PLDs) is an important quantity that can be determined from measurements of the CR composition at Earth. It determines the number of spallation reactions that a typical primary CR undergoes, that can be measured by using the ratio of fluxes of secondary-primary nuclei, like Boron to Carbon ratio. In our calculation the path length increases by  $\delta \ell = v \Delta t$  over a time span  $\Delta t$ , with  $v$  the instantaneous CR velocity. The grammage increases as:

$$\Delta \Sigma_{cr} = \rho(\mathbf{r}_{cr}) v \Delta t, \text{ with } \rho(\mathbf{r}) = \begin{cases} \rho_0 \exp(-|z|/H_d(r)) & \text{for } r < R_c, \\ \rho_0 \exp(-|z|/H_d(r)) \exp[-(r - R_c)/R_d] & \text{for } r > R_c. \end{cases} \quad (5)$$

where  $\rho(\mathbf{r})$  is the density of the diffuse gas at CR position  $\mathbf{r}$ ,  $v \simeq c$  is the velocity of the CR, and  $\mathbf{r}_{cr}$  is the instantaneous position of the CR inside the Galaxy. The radial scale length  $R_c$  in the density distribution equals  $R_c = 7$  kpc. The vertical density scale height  $H_d(r) = H_0 \exp(r/R_h)$ . Here  $R_h \simeq 9.8$  kpc and  $H_0 \simeq 0.063$  kpc.

### 2.4 Model for the Galactic wind

Several theoretical papers e.g: [Breitschwerdt et al. \(1991\)](#), [Zirakashvili et al. \(1996\)](#), and [Pakmor et al. \(2016\)](#) conclude that CRs can play an important role in launching Galactic winds. For instance: [Breitschwerdt et al. \(1991\)](#), and [Breitschwerdt et al. \(1993\)](#) showed that the Galactic winds are accelerated by the pressure of the CRs, as well as by gas- and MHD wave pressure. As a result the wind velocity can reach several hundred km/s. [Everett et al. \(2008\)](#) shows that the initial velocity, close to the disk, is about 200 km/s and increases to 600 km/s.

When CRs couple to the plasma via scattering by MHD waves, the Galactic winds develop and CRs are picked up at the height  $|z| \sim D/V_w$  by the wind with velocity  $V_w$ . They are then transported out of the Galaxy (i.e: CRs will generally not return). Since our simulations propagate test particles in a prescribed magnetic field and/or flow, we can *not* simulate the self-consistent launch of a CR-driven wind. Instead we use a simple analytical model.

The velocity of a steady and axi-symmetric Galactic wind in the MHD approximation must take the form (e.g [Weber & Davis \(1967\)](#)):

$$\mathbf{V}_w = V_p \frac{\mathbf{B}_p}{|\mathbf{B}_p|} + V_{\phi} \hat{\phi} \quad (6)$$

Here  $\mathbf{B}_p$  is the poloidal magnetic field:  $\mathbf{B}_p = (B_r, 0, B_z)$ . In our model we will neglect the motion in the azimuthal ( $\phi$ -)direction since our model (including the CR source distribution) is axially symmetric, retaining only the wind component  $V_p$  along the poloidal field. We do not employ a full model for the Galactic wind. Rather we assume that the poloidal wind speed varies with height  $z$  above the disk as:

$$V_p(z) = V_0 \left( \frac{|z|}{H_w} \right), \quad (7)$$

a reasonable approximation sufficiently close to the disk for a wind accelerating away from the Galactic Disk. We use  $H_w = 20$  kpc in these simulations, and vary  $V_0$  between 0 and 600 km/s. The importance of CR advection by this wind is determined by the dimensionless parameter:

$$\Xi_w = \frac{V_0 H_w}{D_{zz}} \simeq 10 \left( \frac{V_0}{100 \text{ km/s}} \right) \left( \frac{H_w}{10 \text{ kpc}} \right) \left( \frac{D_{zz}}{3 \times 10^{28} \text{ cm}^2/\text{s}} \right)^{-1}. \quad (8)$$

Here  $D_{zz}$  is the  $zz$ -component of the CR diffusion tensor. Advection away from the disk becomes the dominant transport mechanism for CRs when  $\Xi_w \gg 1$ . Of course, in this model (with  $V_p \propto |z|$ ) it is essential that diffusion first transports the CRs some distance away from the disk mid-plane. As an illustration: if the CR is ‘picked up’ by the wind at some height  $h_* \ll H_w$  from the mid-plane, the ratio of the diffusion time  $t_{\text{diff}} = H_w^2/2D_{zz}$  to a height  $H_w$  and the advection time  $t_w = (H_w/V_0) \ln(H_w/h_*)$  to the same height is:

$$\frac{t_{\text{diff}}}{t_w} = \left( \frac{H_w V_0}{2D_{zz}} \right) \left[ \ln \left( \frac{H_w}{h_*} \right) \right]^{-1} = \frac{\Xi_w}{2} \left[ \ln \left( \frac{H_w}{h_*} \right) \right]^{-1}. \quad (9)$$

In practice  $h_*$  will roughly equal the thickness of the stellar disk of the Galaxy,  $h_* \simeq 0.2 - 0.4$  kpc.

## 2.5 Effective drift speed in the Itô formulation

The precise treatment of drift and diffusion needs some discussion. Without scattering, the drift velocity of a charge  $q$  with momentum  $\mathbf{p}$  and velocity  $\mathbf{v}$  in a static magnetic field  $\mathbf{B}(\mathbf{x})$  is a combination of gradient  $B$  drift and curvature drift, which equals (see Appendix A):

$$\mathbf{V}_{\text{gc}} = \frac{cpv}{3q} \nabla \times \left( \frac{\mathbf{B}}{B^2} \right), \quad (10)$$

when averaged over an isotropic distribution of momenta so that  $\langle p_{\perp} v_{\perp} \rangle / 2 = \langle p_{\parallel} v_{\parallel} \rangle = pv/3$ , where the brackets are the average over momentum direction and the subscript  $\perp$  ( $\parallel$ ) refers to the component perpendicular (parallel) to the magnetic field. This is the (slow) drift of the *guiding center*, the average position of the charge when one averages over the rapid gyration around the magnetic field. These drifts are fully discussed in the classic paper of [Northrop \(1961\)](#). The well-know  $\mathbf{E} \times \mathbf{B}$  drift is included in the wind velocity since the MHD condition applies so that  $\mathbf{E} = -(\mathbf{V}_w \times \mathbf{B})/c$ .

The *full* diffusion tensor, in a simple collisional model with collision frequency  $\nu_s$ , takes the form in component notation (e.g. [Miyamoto \(1980\)](#), Ch. 7.3):

$$D_{ij} = D_{\parallel} b_i b_j + D_{\perp} (\delta_{ij} - b_i b_j) - D_a \epsilon_{ijk} b_k. \quad (11)$$

Here  $b_i$  is the  $i$ -th component of the unit vector  $\hat{\mathbf{b}}$  of the ordered magnetic field, and  $\epsilon_{ijk}$  is the totally anti-symmetric symbol in three dimensions. The three fundamental diffusion coefficients appearing in this expression are:

$$D_{\parallel} = \frac{v^2}{3\nu_s}, \quad D_{\perp} = D_{\parallel} \left( \frac{\nu_s^2}{\nu_s^2 + \Omega^2} \right), \quad D_a = D_{\parallel} \left( \frac{\nu_s \Omega}{\nu_s^2 + \Omega^2} \right). \quad (12)$$

Here  $\Omega = qB/\gamma mc$  is the gyration frequency of the charge with  $\gamma = 1/\sqrt{1 - v^2/c^2}$  its Lorentz factor. When this diffusion tensor is used in the diffusion equation the term involving  $D_a$  leads to an advection term (and not to a diffusion term because of the anti-symmetry of this term in the indices  $i$  and  $j$ ), with an effective guiding center drift velocity equal to:

$$\mathbf{V}_{\text{gc}} = \frac{cpv}{3q} \nabla \times \left\{ \frac{\Omega^2}{\nu_s^2 + \Omega^2} \left( \frac{\mathbf{B}}{B^2} \right) \right\}. \quad (13)$$

In our simple model we assume that  $D_{\perp}/D_{\parallel} \equiv \epsilon$  is a constant, where (12) then yields  $\epsilon = \nu_s^2/(\nu_s^2 + \Omega^2)$ . Then, in order to be consistent, the guiding center drift velocity must be defined as:

$$\mathbf{V}_{\text{gc}} = (1 - \epsilon) \frac{cpv}{3q} \nabla \times \left( \frac{\mathbf{B}}{B^2} \right). \quad (14)$$

It reduces to the standard (collisionless) form when  $\epsilon \ll 1$  ( $\nu_s \ll \Omega$ ) and vanishes for  $\epsilon = 1$ , the case of isotropic diffusion. This is physically correct.

The diffusive random step  $\Delta \mathbf{x}_{\text{diff}}$  in (3) only involves  $D_{\parallel}$  and  $D_{\perp}$ , the two diffusion coefficients that determine the symmetric part of the diffusion tensor that can be written in dyadic notation as  $\mathbf{D}_{\text{symm}} \equiv D_{\parallel} \hat{\mathbf{b}}\hat{\mathbf{b}} + D_{\perp} (\mathbf{I} - \hat{\mathbf{b}}\hat{\mathbf{b}})$ . If there are gradients in the field direction or in the coefficients  $D_{\parallel}$  and  $D_{\perp}$  one must -in the Itô formulation (3) of the equations- include the gradient drift velocity equal to:  $\mathbf{V}_{\text{gr}} = \nabla \cdot \mathbf{D}_{\text{symm}}$ . The total drift velocity  $\mathbf{V}_{\text{dr}} = \mathbf{V}_{\text{gr}} + \mathbf{V}_{\text{gc}}$  becomes, writing the diffusion tensor as the sum of the symmetric and the anti-symmetric part  $\mathbf{D} \equiv \mathbf{D}_{\text{symm}} + \mathbf{D}_{\text{a}}$ :

$$\mathbf{V}_{\text{dr}} = \nabla \cdot \mathbf{D}_{\text{symm}} + (1 - \epsilon) \frac{cpv}{3q} \nabla \times \left( \frac{\mathbf{B}}{B^2} \right) = \nabla \cdot (\mathbf{D}_{\text{symm}} + \mathbf{D}_{\text{a}}). \quad (15)$$

This is the ‘standard form’ found in the mathematical literature on the the Itô formulation. In Appendix A we give explicit analytical expressions for the drift velocity in our adopted magnetic field.

### 3 RESULTS OF THE SIMULATIONS

We present results from our simulations for two different values of the ratio:  $\epsilon = D_{\perp}/D_{\parallel}$ :  $\epsilon = 0.01$  (strongly anisotropic diffusion) and  $\epsilon = 0.5$  (mildly anisotropic diffusion). The diffusion coefficients  $D_{\perp}$  and  $D_{\parallel}$  are kept constant for a given CR energy.

#### 3.1 The effect of the drift

Figure 1 shows the position of CR protons, projected onto the Galactic plane, at the moment they reach the upper (lower) boundary of the CR halo, located at  $z = +H_{\text{cr}}$  ( $z = -H_{\text{cr}}$ ) with  $H_{\text{cr}} = 4$  kpc, or when they reach the outer radius of the Galaxy, taken to be  $r_{\text{max}} = 20$  kpc. In these simulations there is no Galactic wind. All CRs were injected at  $(X, Y) = (7 \text{ kpc}, 0)$ .

For strongly anisotropic diffusion ( $D_{\perp}/D_{\parallel} = 0.01$ , the left two panels) the CRs are mostly follow the spiral field. In the mildly anisotropic case ( $D_{\perp}/D_{\parallel} = 0.5$ , the right two panels) CRs spread out almost isotropically from the injection site. In the two top panels the drift motion is neglected. In the bottom two panels the drift motion is taken into account. Without drift, CR protons spread over a larger region of the disk before escaping. The drift motion leads to a faster escape of CRs, and as a result compresses the distribution of the CRs. It also leads to a bulk inward drift to smaller radii. As the effective drift velocity is proportional to  $\epsilon - 1$ , the effect of drift is smaller for the case  $\epsilon = 0.5$ .

Figure 2 (left column) shows the distribution of the CRs of Figure 1 over the accumulated grammage, calculated at the moment of escape from the Galaxy. In the red histogram the drift motion is neglected, while in the blue histogram the drift motion is taken into account. The right column of Figure 2 shows the grammage distribution of these CRs observed around the Solar System, without (in red) and with (in blue) drift.

Without drift, the accumulated grammage is larger as CRs spend more time in the CR halo. This allows them to spread out over a larger range in galactic radius before they escape. This agrees with the spatial distribution (projected onto the Galactic disk) shown in Figure 1. In conclusion: given  $D_{\parallel}$  and  $\epsilon$ , the drift significantly decreases the residence time in the CR halo.

#### 3.2 CR advection by a Galactic wind

Figures 3 through 5 show the effect of CR advection by a Galactic wind. The  $D_{\parallel}$  in these simulations is kept constant at  $D_{\parallel} = 3 \times 10^{28} \text{ cm}^2 \text{ s}^{-1}$ . The wind velocity is taken to increase linearly with height  $|z|$  away from the disk mid-plane, see prescription (7). The resulting CR transport is diffusive close to the Galactic disk. It becomes convective further out, i.e. there is a strongly diminished chance that CRs return to the mid-plane of the Galactic disk. We then extend the CR halo to a height  $H_{\text{cr}} = H_{\text{w}} = 20$  kpc in these simulations.

Figure 3 (left column) shows the position of 1 GeV CR protons projected onto the Galactic plane at the moment of escape. The left row is for  $D_{\perp}/D_{\parallel} = 0.01$  and the right row for  $D_{\perp}/D_{\parallel} = 0.5$ . The CRs were injected at  $(X, Y) = (7 \text{ kpc}, 0)$ . We

use three different velocities (see Eqn. 7):  $V_0 = 600$  km/s (upper plot), 200 km/s (middle plot), and 0 km/s (lower plot). In all cases one sees outward CR transport, along the X-field lines perpendicular to the disk. Comparing the top two plots with the wind-less bottom plot it is evident that, with a wind, CRs escape sooner and -as a consequence- fan out less in both the radial and azimuthal directions. While in the right column the effect of the wind is much less evident.

Figure 4, left column, shows the normalized distribution in the age (residence time) of the CR protons at the moment they escape the Galaxy. The right column shows the normalized distribution over the age of the CR protons that observed in the local volume of 1 kpc radius around the Solar System.

In Figure 5 we show the average CR age at the moment of escape as a function of wind velocity (first row). The second row we show the average CR age as a function of  $\Xi_w$  as defined in Eqn. (8). Now CRs are injected over the entire Galactic disk. The CRs are given a weight  $\propto N_{\text{snr}}(r_{\text{inj}})$ , with  $r_{\text{inj}}$  the injection radius and  $N(r)$  is the Galactic surface density of supernova remnants, taken to be the sources of these CRs. We employ the SNR surface density given by Case & Bhattacharya (1996):

$$N_{\text{snr}}(r) \propto \left(\frac{r}{R_{\odot}}\right)^{\alpha} \exp\left(-\frac{r}{R_{\text{snr}}}\right), \quad (16)$$

where  $R_{\odot} = 8.5$  kpc is the position of the Sun,  $\alpha = 1.1$ , and  $R_{\text{snr}} = 8.0$  kpc.

We employ five values for the characteristic wind speed  $V_0$ : between 0 km/s to 600 km/s. In these simulations we take  $D_{\parallel} = 3 \times 10^{28} \text{ cm}^2 \text{ s}^{-1}$ , and we choose  $D_{\perp}/D_{\parallel} = 0.01$  and  $D_{\perp}/D_{\parallel} = 0.5$ .

As clearly seen the average age of CRs decreases as the wind velocity increases. Even though the escape boundary is now at  $H_{\text{cr}} = 20$  kpc, the typical residence time (shown in figure 5) is still around 1 Myr, comparable to what we find in the simulations without a wind where we put  $H_{\text{cr}} = 4$  kpc. In the pure diffusion case one would expect an increase of the residence time ( $\propto H_{\text{cr}}^2$ ) by a factor  $\sim 16$ . This shows that advection by the wind rapidly becomes important. The same behavior is seen if one plots the average CR age as a function of  $\Xi_w$ . In conclusion: given  $D_{\parallel}$ , increasing the wind velocity leads to a reduction of the CR residence time in the Galaxy.

Finally, in Figure 6 we show the B/C ratio as a function of kinetic energy per nucleon. We used the weighted slab technique using the Path Length Distributions (PLDs) as described in AL-Zetoun & Achterberg (2020). for  $D_{\perp}/D_{\parallel} = 0.01$ . In this Figure, the red curve is without drift motion, the blue curve takes drift motion into account, while the black curve takes the wind velocity into account. The experimental data from AMS-02 (Aguilar et al. 2016), PAMELA (Adriani et al. 2014), CREAM (Ahn et al. 2008), and HEAO3 (Engelmann et al. 1990) are shown for comparison. It is possible to get a satisfactory agreement between our results and observational data. The parallel diffusion coefficient is assumed to scale with CR energy as  $D_{\parallel} = D_0 (\mathcal{R}/1 \text{ GeV}/c)^{\delta}$  with  $\delta = 0.33$ . For the calculation without drift (red curve) we use  $D_0 = 3 \times 10^{28} \text{ cm}^2 \text{ s}^{-1}$ , for the calculation with drift (blue curve) we chose the value of  $D_0 = 6.1 \times 10^{28} \text{ cm}^2 \text{ s}^{-1}$ , and for the calculation with a wind we chose the value of  $D_0 = 2.7 \times 10^{29} \text{ cm}^2 \text{ s}^{-1}$  in order to match the observed B/C ratio at 1 GeV/nucleon.

## 4 CONCLUSIONS

In this paper we have investigated by means of numerical simulations the effect of drift motion, as well as the effect of advection of CRs away from the disc by a Galactic wind on the propagation CRs in the Galaxy. We modified the magnetic field model of Jansson and Farrar, while retaining essential features of this model, such as the spiral structure close to the mid-plane of the Galactic disk. The main results are as follows:

- We show that the drift motion alone affects the transport of CRs in the Galaxy, by compressing the CR distribution and by shifting them inward to smaller Galacto-centric radii;
- We show how a Galactic wind affects the transport of CRs in the Galaxy, by advecting them away from their sources. This significantly reduces (for given  $D_{\parallel}$  and  $\epsilon = D_{\perp}/D_{\parallel}$ ) the residence time in the Galaxy and the accumulated grammage, as expected from simple arguments. This implies that, given the observed grammage derived from observations of (for instance) the B/C ratio, the diffusion coefficient  $D_{\parallel}$  must increase for larger values of the Galactic wind speed in order to reproduce the observations. This implies that the sources contributing to the CR flux at Earth must be closer compared to the case without a Galactic wind.
- Away from the disk the flaring vertical X-field leads to a more rapid (mostly advective) transport of CRs to larger Galacto-centric radii when a wind is present.

- As is the case without drift and wind, the accumulated grammage and the residence time depend strongly on the diffusion ratio  $D_{\perp}/D_{\parallel}$ , as already found in [AL-Zetoun & Achterberg \(2018\)](#) for the case without drift or a wind.

## 5 DATA AVAILABILITY

The datasets generated during and/or analysed during the current study are available from the corresponding author on reasonable request.

## REFERENCES

- AL-Zetoun A., Achterberg A., 2018, [MNRAS](#),  
 AL-Zetoun A., Achterberg A., 2020, [MNRAS](#), 493, 1960–1981  
 Adriani O., et al., 2014, [ApJ](#), 791, 93  
 Aguilar M., et al., 2016, [Physical Review Letters](#), 117, 231102  
 Ahn H. S., et al., 2008, [Astroparticle Physics](#), 30, 133  
 Beck R., Krause M., 2005, [Astronomische Nachrichten](#), 326, 414  
 Breitschwerdt D., McKenzie J. F., Voelk H. J., 1991, [A&A](#), 245, 79  
 Breitschwerdt D., McKenzie J. F., Voelk H. J., 1993, [A&A](#), 269, 54  
 Case G., Bhattacharya D., 1996, [A&AS](#), 120, 437  
 Engelmann J. J., Ferrando P., Soutoul A., Goret P., Juliusson E., 1990, [A&A](#), 233, 96  
 Everett J. E., Zweibel E. G., Benjamin R. A., McCammon D., Rocks L., Gallagher III J. S., 2008, [ApJ](#), 674, 258  
 Hopkins P. F., Quataert E., Murray N., 2012, [MNRAS](#), 421, 3522  
 Jaffe T. R., Leahy J. P., Banday A. J., Leach S. M., Lowe S. R., Wilkinson A., 2010, [MNRAS](#), 401, 1013  
 Jansson R., Farrar G. R., 2012a, [ApJ](#), 757, 14  
 Jansson R., Farrar G. R., 2012b, [ApJL](#), 761, L11  
 Jokipii J. R., Levy E. H., Hubbard W. B., 1977, [ApJ](#), 213, 861  
 Martin C. L., 1999, [ApJ](#), 513, 156  
 Miyamoto K., 1980, *Plasma physics for nuclear fusion*. Cambridge, Mass., MIT Press  
 Northrop T. G., 1961, [Annals of Physics](#), 15, 79  
 Pakmor R., Pfrommer C., Simpson C. M., Springel V., 2016, [The Astrophysical Journal](#), 824, L30  
 Skilling J., 1975, [MNRAS](#), 172, 557  
 Strong A. W., Moskalenko I. V., Ptuskin V. S., 2007, [Annual Review of Nuclear and Particle Science](#), 57, 285  
 Sun X. H., Reich W., Waelkens A., Enßlin T. A., 2008, [A&A](#), 477, 573  
 Weber E. J., Davis Leverett J., 1967, [Astrophys. J.](#), 148, 217  
 Wentzel D. G., 1974, [Annual Review of Astronomy and Astrophysics](#), 12, 71  
 Zirakashvili V. N., Breitschwerdt D., Ptuskin V. S., Voelk H. J., 1996, [A&A](#), 311, 113

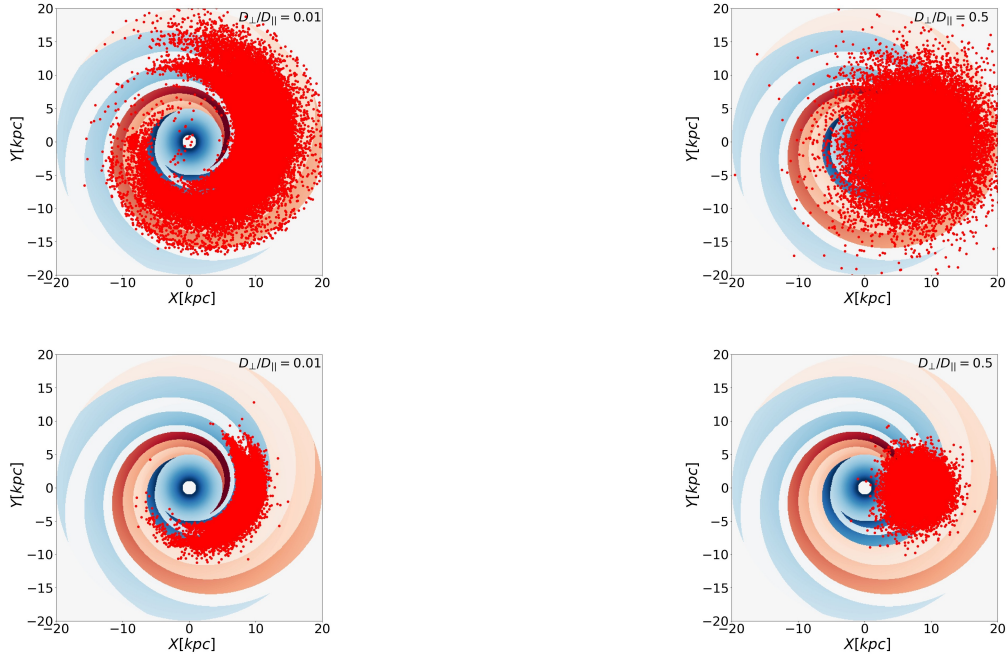


**Figure 1.** The distribution of CR protons projected onto the Galactic plane at the moment of escape. The upper two plots show the results when the drift motion is not considered, in the lower two plots drift motion is taken into account. The right panels are for  $D_{\perp}/D_{\parallel} = 0.01$ , the left panels are for  $D_{\perp}/D_{\parallel} = 0.5$ . In these simulations we take  $D_{\parallel} = 3 \times 10^{28} \text{ cm}^2 \text{ s}^{-1}$ . The CRs were injected at  $(X, Y) = (7 \text{ kpc}, 0)$ .

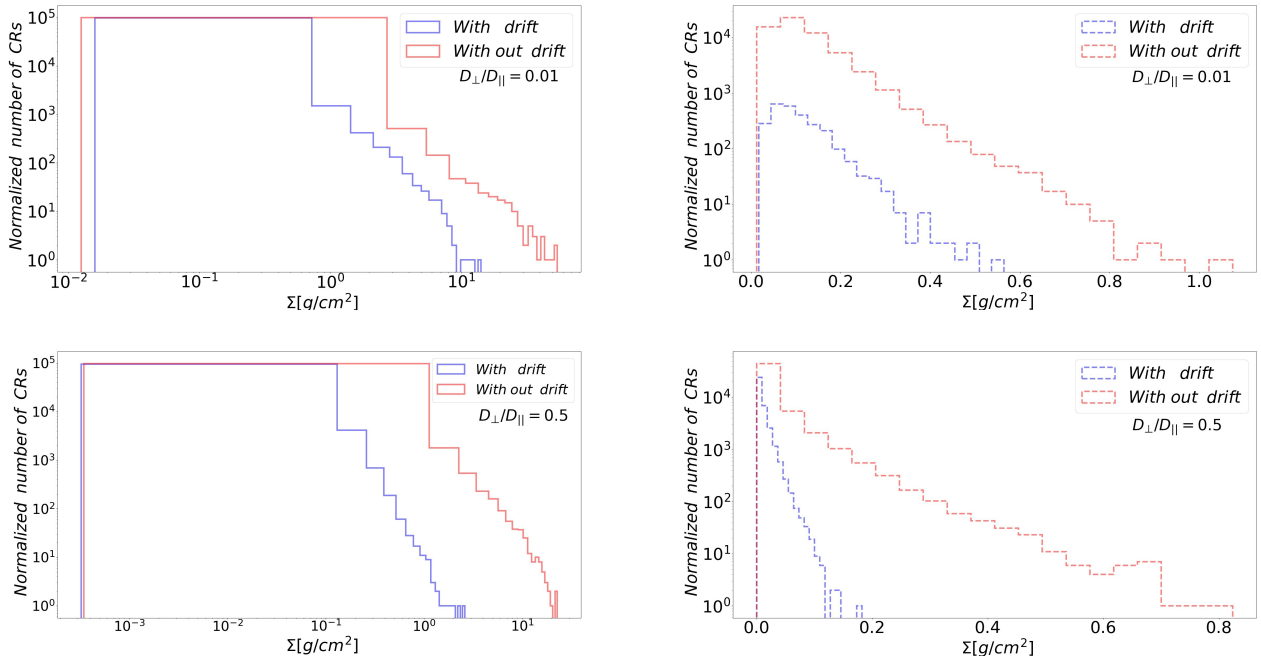


**Figure 2.** The distribution of the accumulated grammage. In the red histograms the drift motion is not considered in the calculation, in the blue histograms the drift motion is taken into account. The left column gives the grammage at the moment of escape, while the right shows it for CRs inside the local volume around the Solar System. Again  $D_{\perp}/D_{\parallel} = 0.01$  and  $D_{\perp}/D_{\parallel} = 0.5$ , as indicated in each panel. As before  $D_{\parallel} = 3 \times 10^{28} \text{ cm}^2 \text{ s}^{-1}$ .



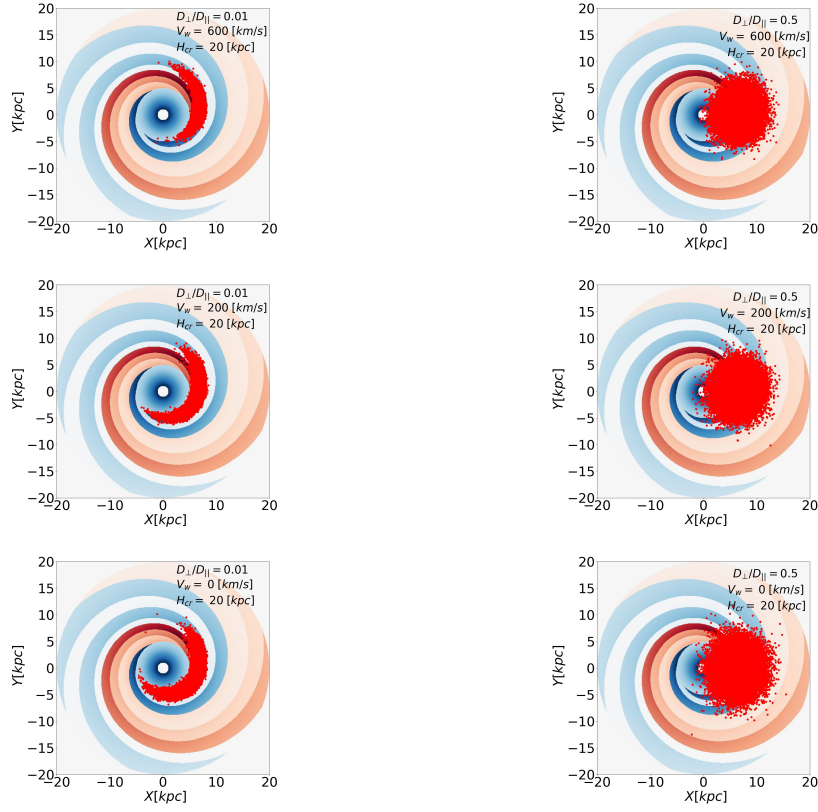


**Figure 3.** The distribution of GCR protons projected onto the Galactic plane for  $D_{\perp}/D_{\parallel} = 0.01$  (left) and  $D_{\perp}/D_{\parallel} = 0.5$  (right). The CRs were injected at  $(X, Y) = (7 \text{ kpc}, 0)$ . The drift motion and a Galactic wind are included in these results. Results are for three different wind velocities, as indicated in each panel, and take  $D_{\parallel} = 3 \times 10^{28} \text{ cm}^2 \text{ s}^{-1}$ .

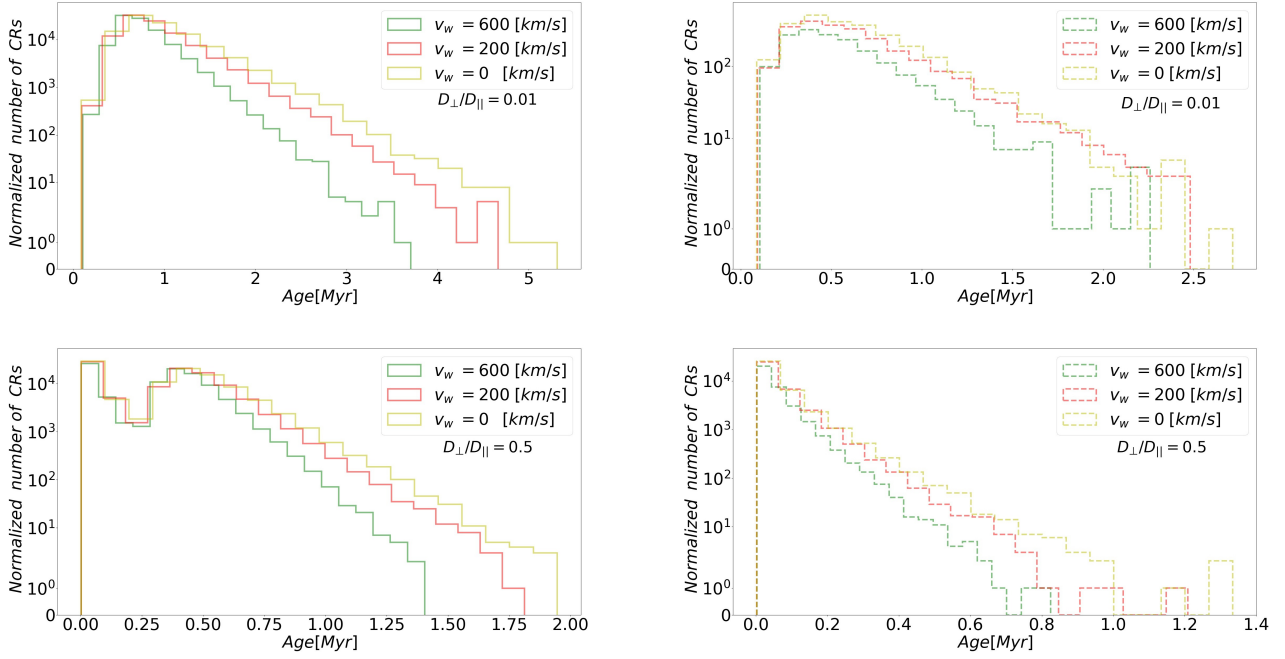


**Figure 4.** The normalized distribution over the age of CRs at the moment of escape from the Galaxy (left column), while in the right column is the normalized distribution over the age of the CRs inside the local volume around the Solar System. The drift motion and the Galactic wind are considered in the calculation. For three different wind velocities, and for  $D_{\perp}/D_{\parallel} = 0.01, 0.5$  as indicated in each panel. And take  $D_{\parallel} = 3 \times 10^{28} \text{ cm}^2 \text{ s}^{-1}$ .

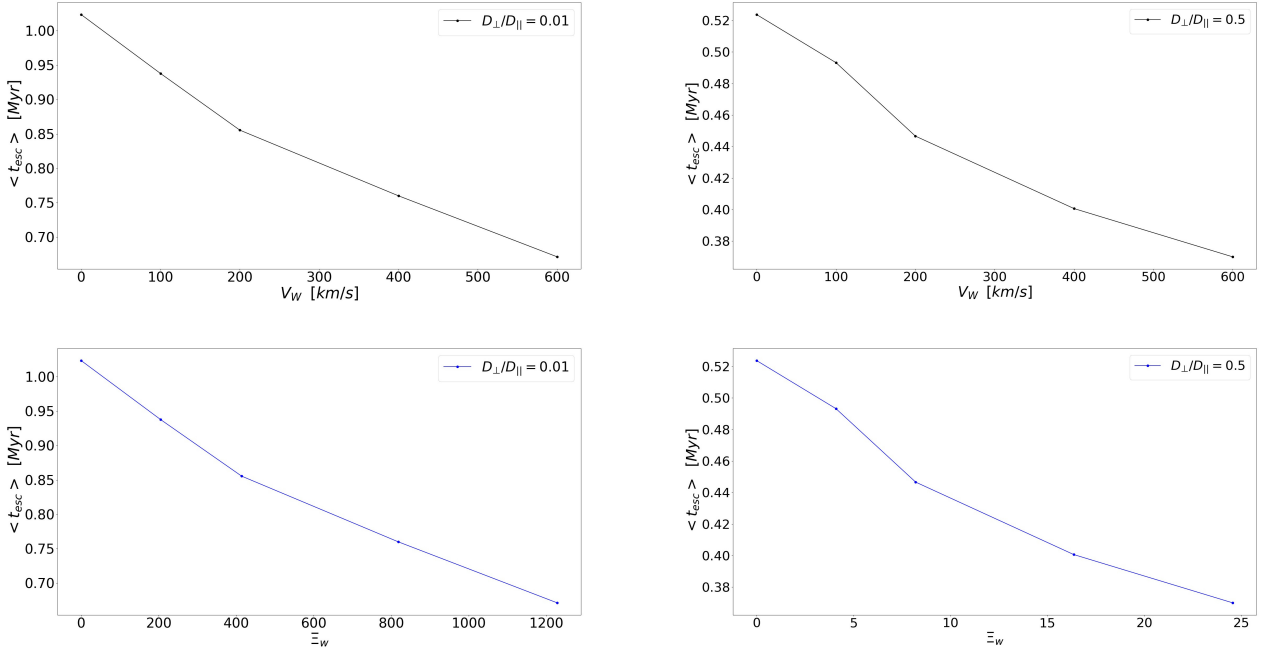


**Figure 5.** The average CR age at the moment of escape as a function of wind velocity (first row). The second row shows the average CR age as a function of  $\Xi_w$ . For five different wind velocities, and for  $D_{\perp}/D_{\parallel} = 0.01, 0.5$  as indicated in each panel. In these simulations we take  $D_{\parallel} = 3 \times 10^{28} \text{ cm}^2 \text{ s}^{-1}$ .

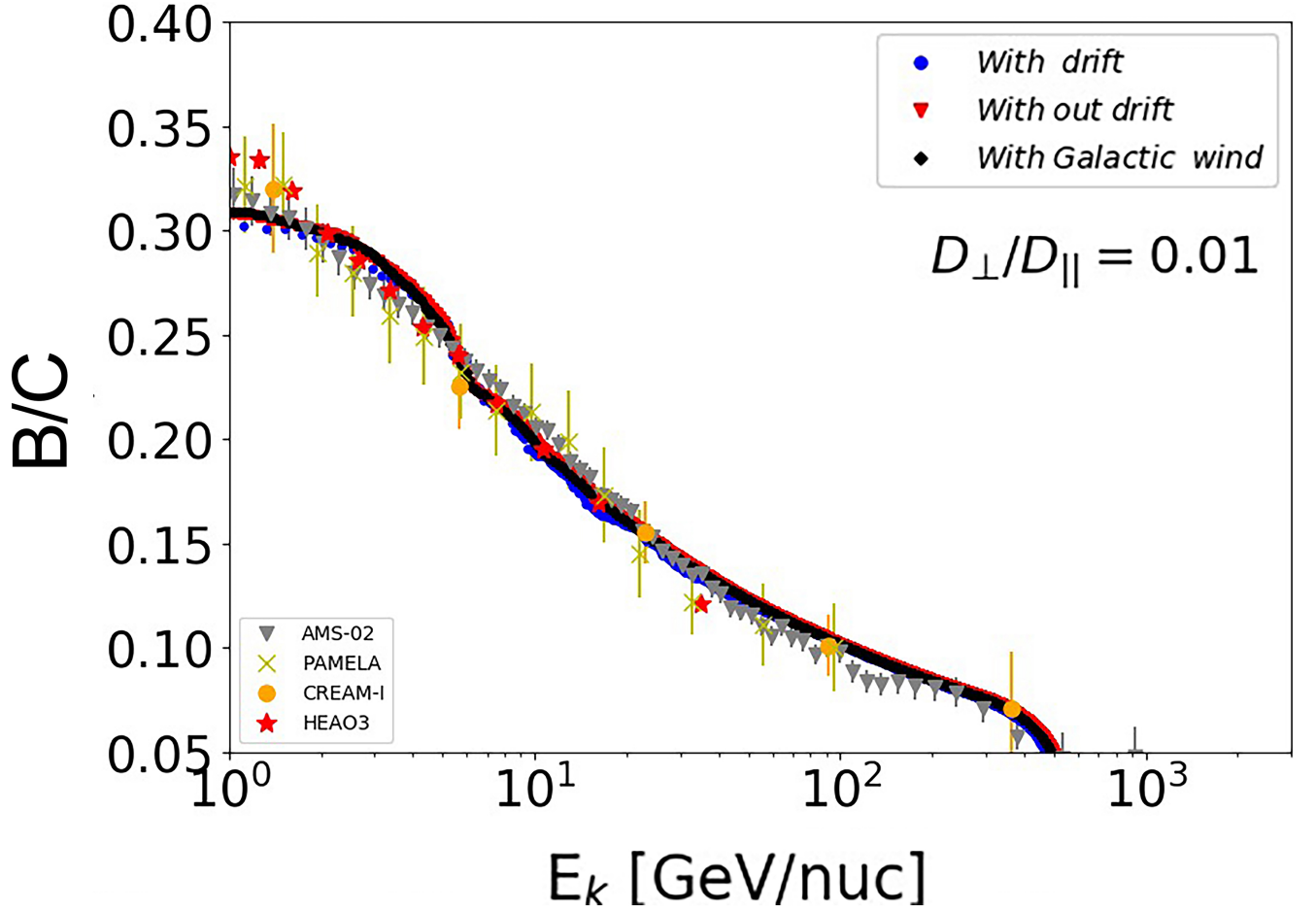


**Figure 6.** The ratio of Boron over Carbon abundance ratio as a function of kinetic energy per nucleon. The gray triangles, yellow crosses, orange points, and red stars are the results of measurements by AMS-02 (Aguilar et al. (2016)), PAMELA (Adriani et al. (2014)), CREAM (Ahn et al. (2008)), and HEAO3 (Engelmann et al. (1990)) respectively. The curves illustrate our results for the case of the diffusion coefficient  $D_{\perp}/D_{\parallel} = 0.01$  once when the drift motion is considered in the calculation (blue curve), the drift motion is not considered in the calculation (red curve), and the wind velocity is considered in the calculation (black curve). We use  $D_0 = 6.1 \times 10^{28} \text{ cm}^2 \text{ s}^{-1}$  for the drift motion (blue curve), with  $D_0 = 3 \times 10^{28} \text{ cm}^2 \text{ s}^{-1}$  when the drift motion is neglected (red curve), and  $D_0 = 2.7 \times 10^{29} \text{ cm}^2 \text{ s}^{-1}$  for the Galactic wind (black curve) to produce the best fit with the observational data.

**APPENDIX A: GUIDING CENTER AND GRADIENT DRIFT VELOCITIES**

We briefly give the analytical results for the drift speeds as they apply in the simplified Jansson-Farrar field employed in this paper.

**A1 Guiding center drift without scattering**

The motion of charged particles with charge  $q$  in a non-uniform magnetic field  $\mathbf{B}(\mathbf{x})$  and a sufficiently weak electric field  $\mathbf{E}(\mathbf{x})$  (with  $|\mathbf{E}| \ll |\mathbf{B}|$ ) can be described as a combination of rapid gyration, fast motion along the magnetic field with velocity  $v_{\parallel}$  and a (slow) drift motion of the guiding center (center of the gyro-orbit). The fast motion along the field is subject to scattering and is taken into account by the parallel diffusion term with diffusion coefficient  $D_{\parallel}$ . Here we concentrate on the slow drift.

If we denote the position of the guiding center by  $\mathbf{R}$ , the drift velocity (to leading order) without scattering equals

$$\left(\frac{d\mathbf{R}}{dt}\right)_{\text{drift}} \equiv \mathbf{V}_{\text{gc}} = c \frac{\mathbf{E} \times \mathbf{B}}{B^2} + \frac{cpv}{3q} \left\{ \nabla \times \left( \frac{\mathbf{B}}{B^2} \right) \right\}. \quad (\text{A1})$$

We assume that there are no other (non-electromagnetic) forces acting on the charge, neglect the polarization drift, which is allowed for slow variations in the electric field. We also take the CR momentum distribution to be isotropic in momentum space. The first term is the well-known  $\mathbf{E} \times \mathbf{B}$  drift. The second term is a combination of the drift due to the gradient of the magnetic field strength, the curvature drift and the parallel drift. As such it is the average over solid angle in momentum space of (see Northrop (1961) for details)

$$\frac{cp_{\perp}v_{\perp}}{2qB^2} (\hat{\mathbf{b}} \times \nabla B) + \frac{cp_{\parallel}v_{\parallel}}{qB} (\hat{\mathbf{b}} \times (\hat{\mathbf{b}} \cdot \nabla) \hat{\mathbf{b}}) + \frac{cp_{\perp}v_{\perp}}{2qB} (\hat{\mathbf{b}} \cdot (\nabla \times \hat{\mathbf{b}})) \hat{\mathbf{b}}. \quad (\text{A2})$$

with  $p_{\perp}$  and  $p_{\parallel}$  ( $v_{\perp}$  and  $v_{\parallel}$ ) respectively the components of momentum (velocity) perpendicular to and along the magnetic field. Then -on average-  $\langle p_{\parallel}v_{\parallel} \rangle = \langle p_{\perp}v_{\perp} \rangle / 2 = pv/3$  and one finds the second term in Eqn. (A1). The  $\mathbf{E} \times \mathbf{B}$  drift is included automatically if one allows for a bulk flow (wind) with velocity  $|\mathbf{V}_w| \ll c$  and uses the ideal MHD condition,  $\mathbf{E} = -(\mathbf{V}_w \times \mathbf{B})/c$ . In that case has to interpret the particle momentum and velocity as those in the local rest frame of the bulk flow, and add the wind speed  $\mathbf{V}_w$  to the (average) CR velocity. This is what we do here. We neglect the small drift that results from the fact that this rest frame is -generally speaking- not an inertial frame.

**A2 Guiding center drift with scattering**

As argued in the main paper the guiding center drift involves a reduced effective drift velocity

$$\mathbf{V}_{\text{gc}} = (1 - \epsilon) \frac{cpv}{3q} \left\{ \nabla \times \left( \frac{\mathbf{B}}{B^2} \right) \right\}, \quad (\text{A3})$$

when scattering is important, with  $\epsilon = D_{\perp}/D_{\parallel}$ . This velocity can be rewritten as

$$\mathbf{V}_{\text{gc}} = (1 - \epsilon) \frac{cpv}{3qBr} \mathbf{\Delta}_{\text{gc}}, \quad (\text{A4})$$

where the dimensionless vector  $\mathbf{\Delta}_{\text{gc}}$  equals

$$\mathbf{\Delta}_{\text{gc}} = Br \left\{ \nabla \times \left( \frac{\mathbf{B}}{B^2} \right) \right\}. \quad (\text{A5})$$

If we define a typical gyroradius by  $r_g = pc/qB$ , the factor in front of  $\mathbf{\Delta}_{\text{gc}}$ , which determines the typical guiding center speed, can be written as

$$(1 - \epsilon) \frac{cpv}{3qBr} = (1 - \epsilon) \left[ \frac{v}{3} \left( \frac{r_g}{r} \right) \right]. \quad (\text{A6})$$

### A3 Gradient drift

For constant  $D_{\parallel}$  and  $D_{\perp}$  there is a gradient drift due to changes in the direction of the magnetic field. The associated velocity  $\mathbf{V}_{\text{gr}} = \nabla \cdot \mathbf{D}_{\text{symm}}$  is

$$\mathbf{V}_{\text{gr}} = D_{\parallel}(1 - \epsilon) \nabla \cdot (\hat{\mathbf{b}} \hat{\mathbf{b}}) . \quad (\text{A7})$$

It can be written as

$$\mathbf{V}_{\text{gr}} = (1 - \epsilon) \left[ \frac{v}{3} \left( \frac{\lambda_s}{r} \right) \right] \Theta , \quad (\text{A8})$$

with the dimensionless vector  $\Theta$  defined as

$$\Theta = r \nabla \cdot (\hat{\mathbf{b}} \hat{\mathbf{b}}) = r (\mathbf{B} \cdot \nabla) \left( \frac{\mathbf{B}}{B^2} \right) . \quad (\text{A9})$$

Here we used  $D_{\parallel} = \lambda_s v / 3$  with  $\lambda_s = v / \nu_s$  the parallel scattering length, employed  $\hat{\mathbf{b}} = \mathbf{B} / B$  and  $\nabla \cdot \mathbf{B} = 0$ . The factor in front of  $\Theta$  in relation (A8) gives the typical magnitude of the gradient drift speed. Comparing this with the guiding center drift speed (A6) one finds that

$$\frac{|\mathbf{V}_{\text{gr}}|}{|\mathbf{V}_{\text{gc}}|} \simeq \frac{\lambda_s}{r_g} . \quad (\text{A10})$$

The two speeds have a similar magnitude when the parallel scattering mean-free-path becomes comparable with the gyro radius, the case of *Bohm diffusion* where CR diffusion is almost isotropic. Strongly anisotropic diffusion occurs when  $\lambda_s \gg r_g$ , in which case  $|\mathbf{V}_{\text{gr}}| \gg |\mathbf{V}_{\text{gc}}|$ .

### A4 Velocities in the simplified JF field

Table A1 below give the parameters needed to calculate the guiding center drift and the gradient drift. It lists the components of  $\Delta_{\text{gc}} \equiv (\Delta_r, \Delta_{\phi}, \Delta_{\theta})$  and of  $\Theta \equiv (\Theta_r, \Theta_{\phi}, \Theta_z)$ . The table lists the results for  $z \geq 0$ . For  $z < 0$  both  $\Delta_z$  and  $\Theta_z$  have the opposite sign. In these expressions we use for  $|z| \leq h$  the parameters  $B_D = B_{D0}(r/r_0)$  and  $B_X(r) = (B_0^X \sin i) \exp(-r_p/H_X)$  and  $B = \sqrt{B_D^2 + B_X^2}$ . The value of  $B_{D0}$  at  $r_0 = 5$  kpc is listed in Table 1 of Jansson & Farrar (2012a) for all the spiral sections of the disk field. Also:  $B_0^X = 4.6 \mu\text{G}$ . The inclination angle  $i$  of the X-field and the radius  $r_p$  have been defined above. Again for  $|z| \leq h$  we define the quantity

$$\Lambda(r, r_p) \equiv -\frac{r}{B_z} \frac{dB_z}{dr} = \begin{cases} \frac{r_p}{H_X} + \cos^2 i & \text{for } r_p \leq r_X, \\ \frac{r}{H_X} & \text{for } r_p > r_X. \end{cases} \quad (\text{A11})$$

The length parameters appearing in Table A1 are:  $h = 0.4$  kpc,  $H_X = 2.9$  kpc and  $r_X = 4.8$  kpc, taken from Jansson & Farrar (2012a) and Jansson & Farrar (2012b).

<b>Table A1</b>		
Parameters for the drift calculation: $ z  \leq h = 0.4$ kpc		
	$r_p \leq r_X$	$r_p > r_X$
$\Lambda(r, r_p)$	$\left(\frac{r_p}{H_X} + \cos^2 i\right)$	$\frac{r}{H_X}$
$\Delta_r$	0	0
$\Delta_\phi$	$-\frac{2B_X}{B} \times \left\{ \left(\frac{B_D}{B}\right)^2 + \Lambda(r, r_p) \left[\left(\frac{B_X}{B}\right)^2 - \frac{1}{2}\right] \right\}$	
$\Delta_z$	$\frac{2B_D \cos p}{B} \times \left\{ \left(\frac{B_D}{B}\right)^2 + \Lambda(r, r_p) \left(\frac{B_X}{B}\right)^2 \right\}$	
$\Theta_r$	$2 \left(\frac{B_D}{B}\right)^2 \left\{ \left[\left(\frac{B_D \sin p}{B}\right)^2 - \frac{1}{2}\right] + \Lambda(r, r_p) \left(\frac{B_X}{B}\right)^2 \sin^2 p \right\}$	
$\Theta_\phi$	$\frac{2B_D^2 \sin p \cos p}{B^2} \left\{ \left(\frac{B_D}{B}\right)^2 + \Lambda(r, r_p) \left(\frac{B_X}{B}\right)^2 \right\}$	
$\Theta_z$	$\frac{2B_D B_X \sin p}{B^2} \times \left\{ \left(\frac{B_D}{B}\right)^2 + \Lambda(r, r_p) \left[\left(\frac{B_X}{B}\right)^2 - \frac{1}{2}\right] \right\}$	
Parameters for the drift calculation: $ z  > h = 0.4$ kpc		
	$r_p \leq r_X$	$r_p > r_X$
$\Delta_r$	0	0
$\Delta_\phi$	$-\frac{r_p \sin i}{H_X} (1 + \cos^2 i)$	$-\frac{r \sin i_0}{H_X} (1 + \cos^2 i_0)$
$\Delta_z$	0	0
$\Theta$	$2 \cos i \hat{\mathbf{b}}$	$\cos i_0 \hat{\mathbf{b}}$